Luminescence Quenching of Ru-Labeled Oligonucleotides by Targeted Complementary Strands

D. García-Fresnadillo,*† N. Boutonnet,* S. Schumm,* C. Moucheron,* A. Kirsch-De Mesmaeker,* E. Defrancq,‡ J. F. Constant,‡ and J. Lhomme‡

*Université Libre de Bruxelles, Organic Chemistry and Photochemistry, B-1050 Brussels, Belgium, †Department of Organic Chemistry, Faculty of Chemistry, Universidad Complutense de Madrid, Avenida Complutense s/n, E-28040 Madrid, Spain, and ‡Université Joseph Fourier, Bioorganic Chemistry, LEDSS associated to CNRS, F-38041 Grenoble Cédex 9, France

ABSTRACT The yield of hole injection into guanines of different oligonucleotide duplexes by a photooxidizing tethered Ru(II) complex is examined by measuring the luminescence quenching of the excited complex. This yield is investigated as a function of the anchoring site of the complex (on a thymine nucleobase in the middle of the sequence or on the 5′ terminal phosphate) and the number and position of the guanine bases as compared with the site of attachment of the Ru(II) compound. In contrast to other studies, the tethered complex, $[Ru(tap)_2(dip)]^{2+}$, is a non-intercalating compound and has been shown previously to produce an irreversible photocrosslinking between the two strands as the ultimate step of hole injection. The study of luminescence quenching of the anchored complex by emission intensity and lifetime measurements for the different duplexes indicates that a direct contact between the complex and the guanine nucleobase is needed for the electron transfer to take place. Moreover, for none of the sequences a clear contribution of a static quenching is evidenced independently of the two types of attachment of the $[Ru(tap)_2(dip)]^{2+}$ complex to the oligonucleotide. A comparison of the fastest hole-injection process by electron transfer to the excited anchored $[Ru(tap)_2(dip)]^{2+}$, with the rate of the photo-electron transfer between the same complex free in solution and guanosine-5′-monophosphate, indicates that the hole injection by the anchored complex is slower by a factor of 10 at least. A bad overlap between donor and acceptor orbitals is probably the cause of this slow rate, which could be attributed to some steric hindrance induced by the complex linker.

INTRODUCTION

Ru(II) complexes have been shown to be very useful to probe DNA. The sensitivity of their luminescence to the DNA nucleobases' environment has been exploited in numerous studies for probing several characteristics of DNA extending from its structure or morphology (Pyle and Barton, 1990; Nordén et al., 1996) to the specificity of a sequence (Kirsch-De Mesmaeker et al., 1996; Moucheron et al., 1998; Armitage, 1998; Erkkila et al., 1999). In this context, we have more particularly studied Ru(II) complexes containing highly π-deficient polyazaaromatic ligands, such as tap (1,4,5,8-tetraazaphenanthrene) (Lecomte et al., 1994; Moucheron et al., 1997). The luminescence of these complexes containing at least two tap ligands is quenched by interaction with DNA. This emission inhibition has been demonstrated to originate from a photoinduced electron transfer from a DNA guanine to the excited complex (Kirsch-De Mesmaeker et al., 1996; Moucheron et al., 1998). This charge transfer process does not take place with the adenine nucleobases because the process is not sufficiently exergonic. The electron transfer gives rise to photoadduct formation with the guanine. Nuclear magnetic resonance analyses of this photoadduct have shown that the reaction sphere around the Ru(II) ion remains intact, whereas one of the tap ligands forms an irreversible bond with the amino group of the guanine (Jacquet et al., 1995, 1997; Kelly et al., 1997).

In this work, we have exploited the luminescence and photochemical properties of these complexes by using double-stranded oligonucleotides where one of the strands is labeled, via a linker, with such a tap complex. The goals for studying such synthetic duplexes are manifold. Such systems are interesting in the area of the antisense or antigene strategy to inhibit the function of a gene. The Ru-labeled strand (probe sequence) is, under illumination and after hybridization with its complementary strand (targeted sequence), indeed capable of damaging the targeted sequence by photoadduct formation at a guanine site (Ortmans et al., 1999). We have demonstrated that this process produces an irreversible photo–cross-linking of the two strands. Hence, visible illumination would offer the possibility to cross-link a synthetic Ru-derivatized oligonucleotide irreversibly to its targeted sequence. The use of such photoreactive oligonucleotides would be a serious advantage, as one of the main drawbacks of the antisense or antigene strategy is the instability of the association of the synthetic oligonucleotide with the targeted sequence.

However, the study of such Ru-labeled oligonucleotide duplexes is also useful to explore the electron transfer step from the oligonucleotide duplex to the excited complex. The so-produced holes on DNA are mainly responsible for DNA damages that play a very important role in DNA biology (Breen and Murphy, 1995). These oxidative damages can be repaired by enzymes but are also at the origin of mutations and permanent dysfunction of a gene. The hole

Submitted March 21, 2001 and accepted for publication October 22, 2001.

Address reprint requests to: Dr. A. Kirsch-De Mesmaeker, Université Libre de Bruxelles, Department of Physical Organic Chemistry, CP 160/08, 50 Avenue F. D. Roosevelt, B-1050 Brussels, Belgium. Tel.: 322-650-30-17; Fax: 322-650-36-06; E-mail: akirsch@ulb.ac.be.

0006-3495/02/02/978/10 $2.00

injected by an intercalating organic (Gaspar and Schuster, 1997; Wan et al., 1999; Saito et al., 1995, 1998; Arkin et al., 1997) or metallic photosensitizing agent (Hall et al., 1996) or by photodecomposition of a modified DNA ribose (Meggers et al., 1998; Giese et al., 1999), can migrate on DNA and be trapped on guanine sites. In those studies, the goal was to examine the possibility of hole migration through the DNA or electron transfer mediated by DNA. A recent study (Wan et al., 2000) suggests that even in the case of an electron donor and acceptor that are part of the π-stack, the charge injection to the nearest neighbor base is crucial and depends strongly on the nature of that base.

With the Ru-labeled oligonucleotide duplexes of this work, our goal is to examine the factors that influence the hole injection into the oligonucleotides and this with a photosensitizing complex which is adsorbing in the DNA grooves (Ortmans, 1996; Ortmans et al., 1999) and which does not intercalate. We carried out this study by luminescence-quenching measurements. Such studies have to be performed with complexes chemically tethered to oligonucleotides to control the site of hole injection. Therefore, several different Ru(II) derivatized 17-mer oligonucleotides were examined. A $[Ru(tap)_2(dip)]^{2+}$ complex (dip = 4,7-diphenyl-1,10-phenanthroline) was covalently linked either to a modified thymine at the central position of the sequence or to the phosphate backbone at the 5′-end of the Ru derivatized strand (Figs. 1 and 2). The oligonucleotide duplexes differ mainly by the number of guanines and their position relative to the linkage site.

DRu0 and DRu0′ are the reference sequences that do not contain any guanine, hence where the complex luminescence should not be quenched by electron transfer. DRu1, DRu6, and DRu7 were chosen as first test sequences because they contain stacks of several guanines in the close vicinity of the attached complex. Such systems should thus give rise to well detectable quenching. Actually, DRu1 was also examined previously for photo–cross-linking (Ortmans et al., 1999). DRu4 and DRu5 were selected to test the possibility of quenching by electron transfer mediated by DNA, because in those sequences the guanines should not be reached by the attached complex. DRu2 and DRu3 were chosen to compare the efficiency of quenching by a stack of two guanines in the close vicinity of the anchoring site.

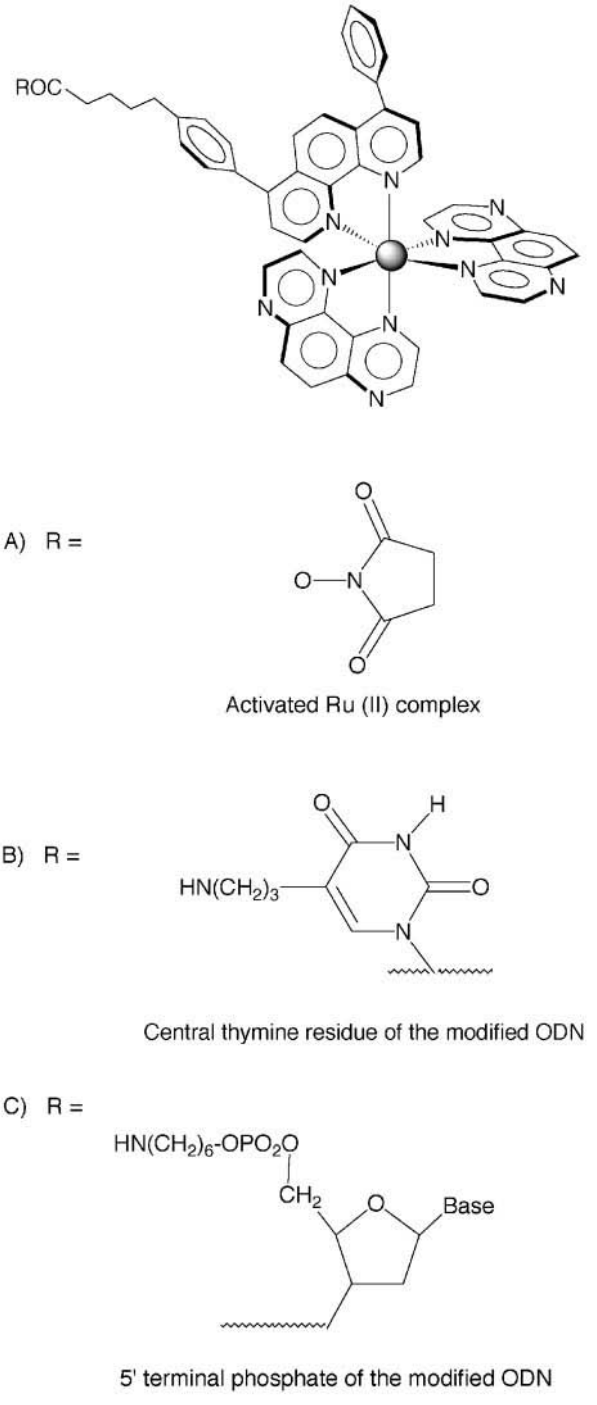

FIGURE 1 Activated $[Ru(tap)_2(dip)]^{2+}$ complex (*A*) and modified oligodeoxyribonucleotides (ODN) with the complex attached in the middle of the strand at position 5 of a thymine (*B*) and at the end of the strand at the 5′-terminal phosphate group (*C*).

Experimental section

The synthesis and purification of the complex $[Ru(tap)_2(dip)]^{2+}$, the preparation of the oligonucleotides, and the coupling procedure between the oligonucleotides and the Ru(II) complex have been reported previously (Ortmans et al., 1999). The main steps of the procedures are as follows.

Complex synthesis

The $[Ru(tap)_2(dip)]^{2+}$ has been prepared by adding 0.2 mmol of the dip ligand derivatized with a pentanoyl carboxylic acid residue to a suspension of 0.15 mmol of the $[Ru(tap)_2Cl_2]$ complex in $EtOH/H_2O$ 1:1. The suspension was refluxed for 36 h under Ar atmosphere and the reaction mixture was filtered, concentrated and treated on a cation exchanger Sephadex SP-C25 column (Amersham Biosciences AB, Uppsala, Sweden) eluted with a NaCl aqueous solution of increasing ionic strength at pH 4.

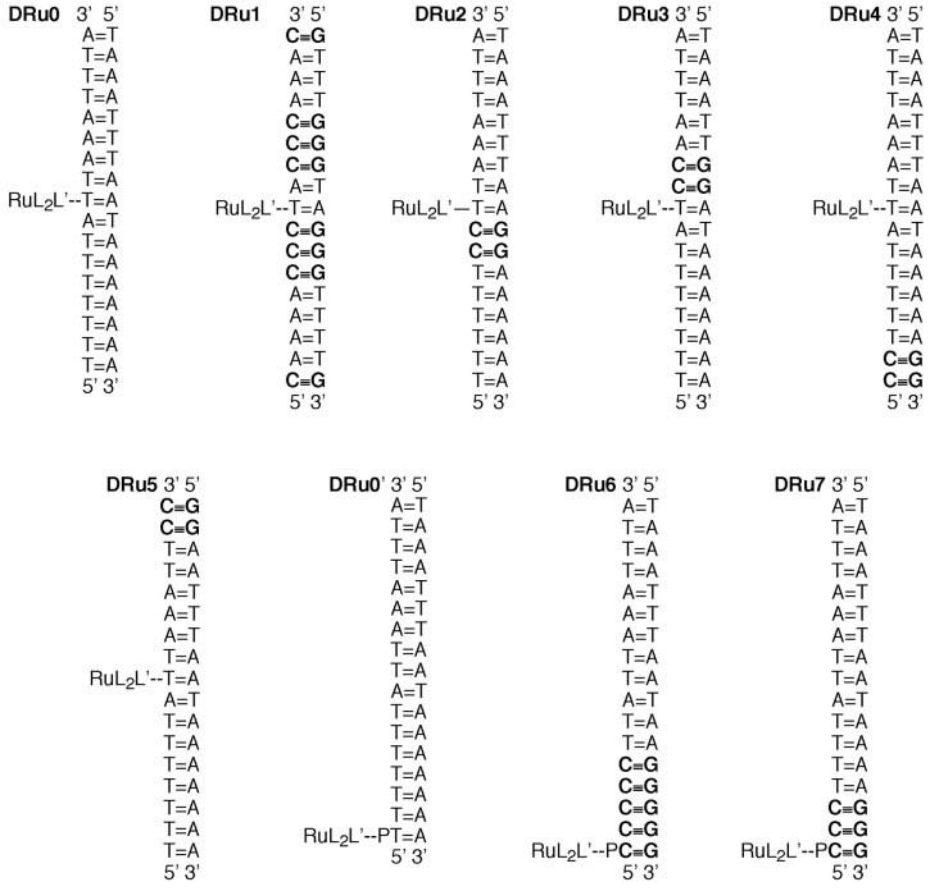

FIGURE 2 The different duplexes sequences. $RuL_2L' = [Ru(tap)_2(dip)]^{2+}$; A, adenine; T, thymine; G, guanine; C, cytosine; P, 5′-terminal phosphate group.

Oligonucleotides synthesis

The modified and unmodified oligodeoxyribonucleotides were synthesized on a controlled pore glass support (1 μmol) by using the phosphoramidite approach on a Perkin-Elmer Expedite DNA synthesizer (Norwalk, CT). The amino-modified oligonucleotides were prepared by using the commercially available aminohexyl phosphoramidite for introduction at the 5′-end, or the phosphoramidite of 5-aminopropyl-2′-deoxyuridine for introduction in the middle of the sequence. At the end of the synthesis of the trityl-protected oligonucleotides, the glass beads were treated with concentrated ammonia at 50°C for 24 h. After lyophilization, the oligonucleotides were purified by high-pressure liquid chromatography, starting with solvent A (ammonium acetate buffer pH 6, 20 mM CH_3CN, 95/5 (v/v)) and applying solvent B (CH_3CN/H_2O, 95/5 (v/v)) up to 30% for 20 min with a flow rate of 4 ml min^{-1}. Treatment with 80% AcOH aqueous solution for 1 h was performed to cleave the trityl protection. The residue after lyophilization was dissolved in water and the aqueous layer was extensively washed with Et_2O. The so-prepared amino-modified oligonucleotides were used without further purification for the coupling reaction with the activated Ru(II) complex.

Coupling reactions

Before its coupling with the deprotected amino-modified oligonucleotides, the Ru(II) complex containing the dip ligand functionalized by the carboxylic acid was activated with *N,N,N′,N′*-tetramethyl(succinimido)uronium tetrafluoroborate. The crude amino-modified oligonucleotide (~0.3 μmol) was dissolved in water (500 μl) in a 2-ml Eppendorf tube (Merck Eurolab, Leuven, Belgium) and *N*-ethyldiisopropylamine (5 μl) was added. A solution of the activated complex (~3 μmol) in *N,N*-dimethylformamide (100 μl) was then added and the reaction mixture was stirred at room temperature in the dark for 12 h. The reaction mixture was then lyophilized. The obtained pellet was suspended in water (500 μl) and the aqueous layer was washed four times with CH_2Cl_2 to remove the excess of unattached $[Ru(tap)_2(dip)]^{2+}$. The Ru-labeled oligonucleotide was then purified by high-pressure liquid chromatography using the same conditions as above. The different $[Ru(tap)_2(dip)]^{2+}$-labeled oligonucleotides were obtained in 50% yield and characterized by electrospray mass spectrometry. Electrospray mass spectrometry for the Ru-derivatized sequences in: DRu0: calcd mass 6077.5, found 6076.2; DRu0′: calcd mass 6213.5, found 6210.7; DRu1: calcd mass 5984.4, found 5982.7; DRu2: calcd mass 6038.5, found 6037.1; DRu3: calcd mass 6038.5, found 6036.5; DRu4: calcd mass 6047.5, found 6047.9; DRu5: calcd mass 6038.5, found 6037.3; DRu6: calcd mass 6138.4, found 6137.8; and DRu7: calcd mass 6168.4, found 6168.4.

Preparation of solutions

The duplex solutions (600 μl) were prepared at a concentration of ~10 μM. The appropriate volume of conjugate in water was dissolved in aqueous buffer (50 mM NaCl, 10 mM Tris, pH 7) and the necessary volume of the complementary strand in water was then added. To ensure formation of the duplexes, a 5–10% excess of the complementary strand

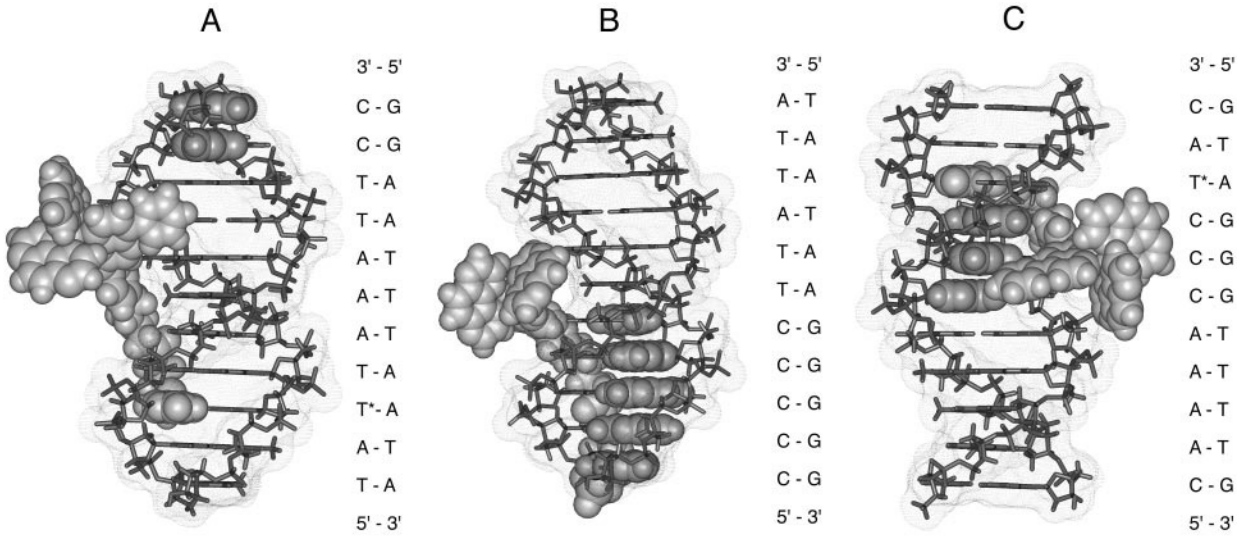

FIGURE 3 Computer models (see Experimental) for the most stretched configurations of the attached complex. The relevant guanines, the modified thymine used to attach the complex, and the complex/linker are shown as space filled models. A Connolly surface calculated for the double stranded oligonucleotide with a probe radius of 1.4 Å is indicated by dots. (*A*): DRu5, stretching toward the 5′-end of the non-Ru-labeled sequence; (*B*): DRu6, stretching toward the 5′-end of the non-Ru-labeled sequence; (*C*): DRu1, stretching toward the 3′-end of the non-Ru-labeled sequence.

was added. The duplex solutions were incubated in a water bath at 90°C for 5 min and the samples were left to equilibrate at room temperature. The samples were stored in the dark at −20°C.

Measurements

All the measurements were carried out in 600-μl quartz cells (1.0 × 0.2 cm) from UV Select (Warrington, UK) and each experiment was performed a minimum of three times with at least two different solutions of each duplex, to test the reproducibility of the experiments. The results were averaged.

Absorption spectra and denaturation curves of the double stranded oligonucleotides were recorded on a Perkin-Elmer Lambda 40 UV/VIS spectrophotometer equipped with a thermostated cell-holder. Temperature was controlled with a Peltier Temperature Programmer PTP-1, DBS Strumenti Scientifici (Padova, Italy). The temperature of the solutions was increased from 10° to 90°C for the duplexes, at a heating rate of 0.5°C min^{-1}. The denaturation curves were analyzed with the UV TempLab software package.

Emission spectra were recorded at room temperature (23 ± 2°C) on a Shimadzu RF-5001PC spectrofluorimeter (Duisburg, Germany) equipped with a Hamamatsu R928 red-sensitive photomultiplier tube (Bridgewater, NJ). Excitation wavelengths were 379 and 422 nm and the spectra were recorded from 500 to 760 nm and from 500 to 800 nm, respectively, and corrected for the photomultiplier response.

Emission lifetimes were measured by using the single-photon counting technique with an Edinburgh Instruments FL900 spectrometer (Edinburgh, UK) equipped with a hypobaric nitrogen-discharge lamp and a Hamamatsu R928 red-sensitive photomultiplier tube. The excitation wavelength was 379 nm and the scattered light was removed with a 420 nm cutoff filter, Coherent-Ealing 26–4267 (Auburn, CA). The emission monochromator was positioned at the maximum luminescence wavelength of each sample (640–650 nm), and 10^4 counts were collected in the peak channel. The temperature of the cell holder was thermostated at 25.0 ± 2.0°C with a Haake NB22 temperature controller (Berlin, Germany). Emission profiles were analyzed with deconvolution of the instrumental response by using the original Edinburgh Instruments software. The decays were fitted from the peak channel to the baseline of the experimental decay. An increasing number of exponentials was used until the fit was statistically acceptable as judged by the χ^2 test (value near 1), the appearance of the weighted residuals plot, the value of the Durbin-Watson parameter, the percentage of weighted residuals <3 standard deviations, and the autocorrelation plot.

Computational models for DRu1, DRu5, and DRu6 were constructed to determine the position of the most distant basepair that can be reached by the complex because of the restrictions imposed by the linker. Instead of the complete 17-mer duplexes, 11-mer subsystems were used to highlight the most important features (i.e., alignment of the complex toward the 3′- or 5′-end). The JUMNA program (Lavery et al., 1995) was used to construct a B-DNA–like three-dimensional model (twist 36°, rise 3.38 Å, inclination 1°, slide, roll, and shift were set to zero). All helical basepair parameters were fixed to the previously mentioned values as the structure of the backbone was relaxed in a molecular mechanics calculation using JUMNA's own FLEX force field. The structure of the complex and the linker were calculated at the density functional theory (DFT) level of theory using the mPW1PW (Adamo et al., 1998) functional in combination with the 3–21G(d) basis set. All DFT calculations were performed with Gaussian 98 (Frisch et al., 1998). Insight II (Molecular Simulations Inc., 1998) was used to build models of the complex attached to the model oligonucleotides either via a thymine or the 5′-end of the phosphate backbone (cf. Figs. 1 and 2). The torsional angles around all the single bonds of the linker as well as the single bond that connects the phenyl group of the dip ligand to the phen moiety were adjusted by hand in an iterative fashion to stretch the linker as far as possible along the major groove. The amid group was restricted to structures close to the *trans* or *cis* conformation (±5°). Two different orientations of the complex, one with a tap ligand and one with the free phenyl group of the dip ligand pointing into the major groove were taken into account. Because both orientations of the complex lead to the same result, only one of them is shown in Fig. 3. For structures with the complex adsorbed in the minor groove, it was found that only the basepairs in the vicinity of the linkage site could be reached.

It should be noted that the structures displayed in Fig. 3 represent extreme cases of the linker/complex stretched along the major groove. Because these purely geometrical models are too crude to give a relative

energy of different conformers, it is impossible to conclude that these conformations are populated in solution at room temperature.

RESULTS

The free complex in solution

The $[Ru(tap)_2(dip)]^{2+}$ complex exhibits strong absorption bands in the UV-Vis region [maxima in water at 276 nm (ϵ = 90 000 M^{-1} cm^{-1}) and 418 nm (ϵ = 22 100 M^{-1} cm^{-1})], an emission quantum yield of 3% (λ_{em}^{max} = 652 nm in water) and a long emission lifetime of 550 and 700 ns in air-equilibrated and argon-purged water, respectively; the luminescent properties in 10 mM Tris buffer solution at pH 7, with 50 mM NaCl are the same as in water. The photoelectron transfer from the guanine bases of DNA to the complex is thermodynamically possible as the reduction potential of $[Ru(tap)_2(dip)]^{2+}$ in the excited state is 1.08 V versus saturated calomel electrode (SCE), whereas the oxidation potential of guanosine 5′-monophosphate (GMP) is 0.92 V versus SCE (Lecomte et al., 1995). Hence, the driving force for the electron transfer process from GMP to the excited complex is of the order of −0.16 eV. The presence of this process has been verified experimentally by the detection of monoreduced complex by laser-flash photolysis experiments (Ortmans, 1996). The bimolecular luminescence quenching constant with GMP attributable to this electron transfer process, has a value of 6.9×10^8 M^{-1} s^{-1}, thus close to the diffusion controlled limit. This behavior is quite similar to that of parent complexes containing two tap ligands such as $[Ru(tap)_2(bpy)]^{2+}$ and $[Ru(tap)_2(phen)]^{2+}$ (Lecomte et al., 1995; Ortmans et al., 1998). The affinity of $[Ru(tap)_2(dip)]^{2+}$ for DNA is rather weak (10^3-10^4 M^{-1}; Ortmans, 1996). Therefore, even with a large excess of calf thymus DNA (in equivalent concentration of base pairs) as compared with the complex concentration, it is difficult to shift completely the equilibrium toward the bound complex (with Tris buffer 10 mM and NaCl 50 mM). Of course, the same interaction problem exists for the free complex in the presence of oligonucleotides. Therefore, the Ru-derivatized duplexes of this work offer the important advantage to have a 1/1 ratio for oligonucleotide/complex.

Melting temperatures of the Ru-labeled oligonucleotides duplexes

The range of melting temperature for the denaturation of the duplexes is narrow for all the sequences, typically ~10°C in agreement with the cooperativity expected for denaturation of rather short oligonucleotides (Cantor and Schimmel, 1980). They are collected in Table 1 for the different natural and $[Ru(tap)_2(dip)]^{2+}$-labeled duplex sequences. They correlate well with the number and position of the G-C (or A-T) basepairs within the duplexes (Cantor and Schimmel, 1980). To test the recognition of the respective specific target sequence by the $[Ru(tap)_2(dip)]^{2+}$-labeled probe sequence, the single-stranded Ru2 conjugate was hybridized with the complementary strand of the Ru3 conjugate (4 basepair mismatches). The melting temperature decreased from 40° to 33°C because of the four basepair mismatches near the anchoring site of the Ru(II) complex. It is interesting to note that no difference between the melting temperatures of the corresponding natural and $[Ru(tap)_2(dip)]^{2+}$-labeled duplexes was observed within experimental error (Table 1). This indicates that there is no extra stabilization of the duplex structure after covalent attachment of the Ru(II) complex.

TABLE 1 Melting temperatures of the natural and $[Ru(tap)_2(dip)]^{2+}$-labeled double stranded oligonucleotides*

Duplex	No. of G-C pairs	T_m(natural)	T_m(Ru-labeled)
DRu0	0	40	40
DRu1	8	60	62
DRu2	2	39	39
DRu3	2	40	40
DRu4	2	45	43
DRu5	2	46	43
DRu0′	0	40	36
DRu6	5	46	48
DRu7	3	41	41

*Temperatures in °C. Experimental error ±2°C.

Steady-state emission maxima of the different duplexes

The emission spectra of the $[Ru(tap)_2(dip)]^{2+}$-labeled duplexes are not dependent on the excitation wavelengths (379 and 422 nm); the corresponding maxima are collected in Table 2. They are slightly blue-shifted for all the sequences as compared with the emission maximum of $[Ru(tap)_2(dip)]^{2+}$ in water (652 nm). These shifts indicate that the double-stranded oligonucleotides provide to the complex a less polar environment than an aqueous solution. Such blue shifts are also observed for the free complex interacting with calf thymus DNA and are ~5 nm. The emission maxima seem to be less blue-shifted for the sequences with the luminophore attached to the 5′-end (DRu0′, DRu6, and DRu7 sequences).

Emission lifetimes of the different duplexes

The emission decay profiles of the different duplexes were fitted to multiexponential functions and the results are collected in Table 2 for air-equilibrated and argon purged solutions (only for the reference sequences). The fact that the decays correspond to multiexponential functions indicates that the attached excited complex probes different types of DNA microenvironments. Moreover, the number of

TABLE 2 Emission maxima and luminescence lifetimes of the $[Ru(tap)_2(dip)]^{2+}$-labeled double-stranded oligonucleotides*

Duplex	λ_{em}^{max}/nm†	$\tau_1/\mu s$‡	$\%C_1$§	$\tau_2/\mu s$‡	$\%C_2$§	$\tau_3/\mu s$‡	$\%C_3$§	$\tau_M/\mu s$¶
DRu0	642	–	–	0.625	29	1.16	71	1.00 ± 0.04
				(0.625)	(25)	(1.20)	(75)	(1.06 ± 0.04)
DRu1	650	0.037	74	0.165	19	0.520	7	0.10 ± 0.02
DRu2	650	0.037	50	0.415	16	0.910	35	0.40 ± 0.01
DRu3	642	0.105	35	0.350	22	0.930	43	0.51 ± 0.03
DRu4	642	–	–	0.620	29	1.19	71	1.03 ± 0.03
DRu5	642	–	–	0.625	32	1.18	68	1.00 ± 0.04
DRu0′	648	–	–	0.545	31	1.00	69	0.86 ± 0.02
				(0.515)	(16)	(1.03)	(84)	(0.94 ± 0.02)
DRu6	650	0.025	68	0.089	21	0.745	11	0.11 ± 0.02
DRu7	646	0.034	79	0.185	7	0.895	14	0.16 ± 0.02

*Luminescence lifetime of the free complex in air-equilibrated and argon-purged solution: 0.550 and 0.700 μs, respectively. λ_{em}^{max} for the free complex in water: 652 nm. All the data are for air equilibrated duplex solution, except the values in parenthesis for argon-purged duplex solutions.

†Experimental error ±2 nm.

‡Decay profiles were fitted to a sum of exponential functions. $I(t) = \Sigma(B_i \exp(-t/\tau_i))$, $(i = 1, 2, 3)$. B_i are the corresponding preexponential factors and τ_i the discrete lifetime components. The experimental errors are the standard deviations (σ_{n-1}) estimated from at least three different measurements. Experimental errors for: biexponential fittings ±10%; triexponential fittings ±10% for τ_3, ±15–20% for τ_1 and τ_2.

§Normalized preexponential factor. $\%C_i = B_i/\Sigma B_i$, $(i = 1, 2, 3)$.

¶Preexponential weighted mean lifetime. $\tau_M = (\Sigma B_i\tau_i)/(\Sigma B_i)$.

exponential decays depends on the absence or presence of luminescence quenching.

In the absence of quenching, when there are no guanine bases in the complementary strand of the conjugate (DRu0 and DRu0′ duplexes) or when the guanines are six basepairs away from the anchoring site of the Ru(II) complex (DRu4 and DRu5 duplexes), the decay profile can be fitted to a biexponential function. The longest lifetime is ~1.2 μs for the duplexes labeled in the middle of the sequence (DRu0, DRu4, and DRu5). The corresponding normalized preexponential factor is ~70%. This factor should be related to the population of excited states with this lifetime, which indicates a rather high population. The long-lived component for the DRu0′ duplex is 1.0 μs with a normalized preexponential factor also of ~70%. These long-lived excited Ru(II) complexes can be attributed to luminophores, which are protected from water by the hydrophobic groove of the double-stranded oligonucleotide (Kirsch-De Mesmaeker et al., 1990). The short-lived components of the decays for the DRu0, DRu4, and DRu5 sequences, where there is no quenching by electron transfer, have a mean value of 625 ns and represent 30% of the excited states. These short-lived species with a lifetime slightly longer than that observed for the free excited $[Ru(tap)_2(dip)]^{2+}$ in water or Tris buffer (550 ns under air) can be attributed to the less protected species that interact with the polyphosphate backbone and not with the hydrophobic bases. For the DRu0′ sequence, the short lifetime component is a bit shorter.

When there are guanines in the vicinity of the attached Ru(II) complex, at least triexponential functions are required to fit the decay profiles (DRu1, DRu2, DRu3, DRu6, and DRu7 duplexes) because of the presence of quenching, which depends on the number of guanine nucleobases. The emission kinetics are quite different compared with those described in the absence of quenching because there are remarkable changes in the τ_i and $\%C_i$ values. The long-lived component is ~920 ns (~40% of the excited states) instead of 1.2 μs. In addition, two short lifetimes can be found, reflecting the presence of luminescence quenching. For the DRu1, DRu6, and DRu7 duplexes, a strong quenching is present as shown by the high contribution of the short-lived components with preexponential factors between 60 and 80%.

Treatment of the lifetimes data in the presence of quenching

When emission decays have to be treated according to triexponential decays, it is difficult to conclude whether the data correspond truly to contributions of three lifetimes and thus three excited species, or whether more lifetimes should be taken into account. Therefore, we have tried a different treatment of these decay kinetics on the basis of the data without quenching. Hence, we have performed a tetraexponential fitting of the emission profiles while fixing the lifetime components at 625 ns and 1.2 μs, values found for the duplexes without quenching (545 ns and 1.0 μs for DRu0′, DRu6, and DRu7, respectively). In this way, we have assumed that for these sequences, the luminophore explores statistically sites where there is no quenching (A-T sites in the groove or sites on the polyphosphate backbone), in addition to guanine sites. Results of this fitting procedure for the duplexes where there is quenching are collected in Table 3. From these fittings, the following conclusions can be drawn. (1) A very short lifetime is obtained for all the sequences (mean value of 16 ns). (2) Although the treatment fixed a lifetime of 1.2 μs, it was not possible to obtain a

TABLE 3 Luminescence lifetimes of $[Ru(tap)_2(dip)]^{2+}$-labeled double stranded oligonucleotides after tetra-exponential fitting*

Duplex	τ_1/ns	% C_1†	τ_2/ns	% C_2†	τ_3/ns	% C_3†	τ_4/ns	% C_4†	τ_M/ns‡
DRu1	16 ± 4	39	61 ± 5	41	625	5	240§	15	100 ± 20
DRu2	16 ± 2	18	44 ± 3	33	625	36	1200	13	400 ± 10
DRu3	8 ± 1	17	118 ± 3	31	625	37	1200	15	450 ± 60
DRu6	16 ± 1	51	56 ± 2	37	545	8	1000	4	110 ± 20
DRu7	18 ± 1	45	57 ± 3	36	545	8	1000	11	180 ± 10

*Decay profiles were fitted to a sum of tetra-exponential functions. $I(t) = \Sigma(B_i \exp(-t/\tau_i))$, $(i = 1, 2, 3, 4)$. B_i are the corresponding preexponential factors and τ_i the discrete lifetime components. The 545 ns, 625 ns, 1.00 μs, and 1.20 μs lifetimes have been fixed.

†Normalized preexponential factor. $\%C_i = B_i/\Sigma B_i$, $(i = 1, 2, 3, 4)$.

‡Preexponential weighted mean lifetime. $\tau_M = (\Sigma B_i\tau_i)/(\Sigma B_i)$.

§The emission decay could not be fitted with a lifetime of 1.20 μs; 240 ns ± 13% is the fourth component of the tetraexponential fitting where only the 625-ns component has been fixed. The experimental errors are the standard deviations (σ_{n-1}) estimated from at least three different measurements.

valuable fitting with such a lifetime for DRu1. This would mean that all the excited species are quenched. (3) The same conclusion can be drawn for the DRu6 duplex for which only a very low contribution of long-lived species is present. This is not the case for DRu7.

Mechanism of quenching

For the duplexes DRu2, DRu3, DRu6, and DRu7 that exhibit a luminescence quenching, one could wonder whether some static quenching would also be present. To verify this hypothesis, the quenching measured from the lifetimes (ratio τ/τ_0) should be compared with that measured from the intensities (ratio I/I_0). For this comparison, one needs to have values for I_0 and τ_0, for references corresponding to duplexes without quenching. However, as two, three, or even four different lifetimes attributable to different microenvironments around the excited complex can be detected depending on the sequence, such a comparison is not straightforward. Recently, a method for assessing the contribution of static quenching in microheterogeneous systems has been developed and successfully applied to many different luminophores interacting with inorganic and organic polymers (Carraway et al., 1991; Xavier et al., 1998; García-Fresnadillo et al., 1999). This method is based on the use of the preexponential weighted mean lifetime, τ_M. This average lifetime is calculated according to Eq 1:

$$\tau_M = \Sigma(B_i \times \tau_i)/\Sigma(B_i) \quad (1)$$

where B_i values are the corresponding preexponential factors and τ_i values are the discrete lifetime components of the multiexponential fitting. It was demonstrated (Carraway et al., 1991) that when using these τ_M values, the absence of static quenching leads to the equality of the ratios in intensities I/I_0 and lifetimes τ/τ_0 as for the homogeneous systems.

TABLE 4 Ratios of emission lifetimes and intensities and % of dynamic quenching for the double stranded $[Ru(tap)_2(dip)]^{2+}$-labeled oligonucleotides*

Sequence	I_i/I_0	τ_M/τ_{M0}†	% Quenching
DRu0	1.00 ± 0.01	1.00 ± 0.01	0
DRu1	0.09 ± 0.01	0.10 ± 0.02	90 ± 10
DRu2	0.42 ± 0.03	0.40 ± 0.01	60 ± 4
DRu3	0.51 ± 0.02	0.51 ± 0.01	49 ± 1
DRu4	1.07 ± 0.02	1.00 ± 0.01	0
DRu5	0.97 ± 0.01	1.00 ± 0.01	0
DRu0′	1.00 ± 0.01	1.00 ± 0.01	0
DRu6	0.13 ± 0.02	0.13 ± 0.02	87 ± 1
DRu7	0.20 ± 0.01	0.19 ± 0.02	81 ± 4

*Air-equilibrated solutions.

†τ_M/τ_{M0} originates from Table 2. The estimated errors are the uncertainties calculated from at least three different measurements.

The τ_M values for the different duplexes are collected in Table 2 for the triexponential fitting, and in Table 3 for the fitting with fixed values. The τ_M values are the same within the experimental error for both types of fitting. These averaged lifetimes reflect properly the extent of quenching affecting each duplex sequence. For the DRu1, DRu2, DRu3, DRu6, and DRu7 duplexes, a moderate or strong luminescence quenching is observed, with the τ_M values ranging from 110 to 510 ns, as compared with 1 μs (for DRu0, DRu4, DRu5) and 860 ns (for DRu0′) when there is no quenching of the complex. The τ_M values for DRu2 and DRu3 show that although the number of guanines is the same, the quenching seems slightly different.

Because of the two different attachments of $[Ru(tap)_2(dip)]^{2+}$ to the duplexes, the two sequences DRu0 and DRu0′ (without guanine) had to be taken as the two reference sequences for the values of I_0 and τ_{M0}. The lifetime and intensity quenching data (I/I_0 and τ_M/τ_{M0}) are collected in Table 4. Within the experimental errors, the ratios in luminescence intensities and lifetimes are the same. Consequently, no static contribution seems to be present in the quenching processes.

Because the $[Ru(tap)_2(dip)]^{2+}$ complex is not very sensitive to quenching by oxygen (Lecomte et al., 1992, 1995) as compared with $Ru(phen)_3^{2+}$ or $Ru(dip)_3^{2+}$ (García-Fresnadillo et al., 1996), the oxygen effect (solution under air and argon-purged) has been tested only with the reference duplexes DRu0 and DRu0′ (Table 2). As indicated by the slight increase of τ_M for the deoxygenated solution (6% increase for DRu0 and 9% increase for DRu0′), the effect of oxygen seems indeed not to be important.

Discussion

The tethering of the $[Ru(tap)_2(dip)]^{2+}$ complex to the double-stranded oligonucleotides does not seem to influence the

melting temperature of the duplexes. Different factors could contribute to this negligible effect of the attached complex. Although the free tap complexes increase the melting temperature of polynucleotides at low ionic strength (Kelly et al., 1987), the T_m increase should be less in the present conditions of higher salt concentration. Moreover, although the complex is tethered to the duplex, its linker could prevent it from adopting a more favorable geometry of interaction within the DNA grooves.

From the inspection of the data in Tables 2, 3, and 4, certain conclusions can be drawn concerning the different sequences.

DRu4 and DRu5

For the duplexes DRu4 and DRu5, no quenching attributable to electron transfer is detected. Hence, an electron transfer among the two guanines at the 5′- or 3′-end of these duplexes and the excited complex is not possible. These guanines are separated by six basepairs from the site of attachment of the complex. We have tried to build computational models where the complex is attached in the middle of the DNA strand. Such models were constructed to determine the position of the most distant basepair which can be reached by the complex with the restrictions imposed by its linker. The computational method is described in the experimental section. In this extreme situation, two different interaction geometries of the complex have been taken into account, one with a tap ligand (not shown) pointing into the major groove and one with the phenyl group of the dip ligand in contact with the major groove (Fig. 3 *A* for DRu5). From these pictures for DRu5, the same conclusion can be drawn for both geometries. The complex is, at least in principle, able to touch a base which is six basepairs away from its linkage site but can not get into direct contact with one or two terminal guanines of this sequence. As no quenching by electron transfer was observed for DRu5 (nor for DRu4), we conclude that a direct contact between a guanine and the complex is a necessary condition for the photoinduced electron transfer to take place. An electron transfer mediated by A-T basepairs is thus not possible.

DRu2 and DRu3

For the duplexes DRu2 and DRu3, with the same type of attachment in the middle of the sequence, there is a non-negligible contribution of the long luminescence lifetime (1.2 μs in Table 3) attributed to the excited complex in contact or in the microenvironment of A-T basepairs, which is indeed logical for both sequences. However, the quenching by the two guanines is a bit more important for DRu2 than DRu3. Obviously, in both cases the complex can reach the stack of two guanines. The difference of quenching measured for the two sequences could be attributed to a difference of ionization potential (IP) (Schumm et al., to be published) for the guanine doublets that are in two different stacking environments. For DRu2, thus for the sequence 3′-AAGGAA-5′, the calculated IP (HF/6–31G(d)) is 6.32 eV, whereas for DRu3, thus for the sequence 3′-TAGGTT-5′, the calculated IP is 6.42 eV. These IP calculations are in agreement with the percentage of quenching because DRu2 gives a quenching of 60% (lower IP) whereas DRu3 gives a quenching of 49%.

DRu6 and DRu7

As mentioned in the introduction, DRu6 and DRu7 have been designed to test the efficiency of quenching with the attachment to the 5′-position of the phosphate. Five guanines have been inserted to increase the chances to observe a well measurable quenching. The situation with this type of tethering could indeed be different than with the attachment in the middle of the sequence on position 5 of a thymine. Because the affinity of the free $[Ru(tap)_2(dip)]^{2+}$ complex for DNA is rather low (Ortmans, 1996), and because the attachment is at the level of the phosphate backbone, one could wonder whether the complex would have a sufficiently high affinity to interact with the guanines in the grooves. This type of tethering could lead to a different situation compared with the case of the attachment in the middle of the sequence in the hydrophobic environment of the major groove. However, despite this low affinity, as shown by the presence of quenching for the DRu6 and even for the DRu7 sequence, the complex interacts with the duplex. For the same attachment on the terminal phosphate for the reference sequence DRu0′, τ_M of the excited complex (860 ns) is shorter than τ_M of DRu0 (1000 ns) (Table 2); the same trend is observed for the longest lifetime component of these two reference duplexes. The slightly shorter lifetimes for DRu0′ than for DRu0 could be attributed to the fact that the complex attached to the terminal phosphate, because of its low affinity for DNA and because of the different linker, is on the average less protected from the aqueous environment than for the complex tethering in the groove in the middle of the duplex. The slight increase of sensitivity to oxygen and the less important blue-shift in absorption for DRu0′ as compared with DRu0 (Table 2) would be in agreement with this conclusion.

The weak contribution of the lifetime of 1 μs in DRu6 which increases in DRu7 (Table 3) indicates that the complex can reach the A-T bases, six and four basepairs away from the site of the modified phosphate in DRu6 and DRu7, respectively. As shown by the computer model in Fig. 3 *B* for DRu6, the complex can indeed reach, when the linker is completely stretched in the major groove, the sixth and seventh base pair (A-T sites) from the attachment at the 5′-terminal phosphate.

As already mentioned, for none of the sequences examined has a static quenching been evidenced, even for DRu6

where there is a stack of five guanines for which the IP is lowered as compared with a guanine doublet or GMP (Sugiyama and Saito, 1996; Schumm et al., to be published). The exergonicity of the electron transfer from this stack of five guanines in DRu6 should thus be higher than with GMP. However, it is striking to observe that the corresponding rate constant does not seem to increase with this exergonicity. Indeed, the quenching rate constant k_q for the quenching of excited $[Ru(tap)_2(dip)]^{2+}$ by GMP is $7 \times 10^8\ M^{-1}\ s^{-1}$. This is not far from a diffusion-controlled process which for $Ru(tap)_3^{2+}$ and GMP reaches $1 \times 10^9 M^{-1}s^{-1}$ (Lecomte et al. 1992). We could thus admit in a first approximation that the electron transfer with GMP is diffusion controlled, so that $k_{e.t.}$ with GMP should be faster. Consequently, as the stack of five guanines in DRu6 has a lower IP than GMP, the electron transfer rate should still be faster. This does not seem to be true, as the fastest quenching process in this sequence is 1/16 ns $= 6 \times 10^7\ s^{-1}$, which is rather slow (Table 3). The same conclusion can be reached if we make another approximation for the quenching with GMP, i.e., if we assume that k_q for excited $[Ru(tap)_2(dip)]^{2+}$ by GMP is not controlled by diffusion but by the electron transfer process. In such a case, k_q can be approximated by $k_q \sim (k_d/k_{-d}) \times k_{e.t.} \sim k_{e.t.} \sim 7 \times 10^8\ s^{-1}$ (where k_d/k_{-d} are the rate constants for the formation and dissociation of the encounter complex by diffusion and $k_{e.t.}$ is the rate constant of electron transfer). A value of $7 \times 10^8\ s^{-1}$ for $k_{e.t.}$ with GMP is again faster than the fastest rate constant measured for DRu6, i.e., $6 \times 10^7\ s^{-1}$. To explain this slow rate with DRu6, we have to conclude that, because of steric hindrance brought by the attachment of the complex, the overlap and orientation of the donor orbital(s) of guanine relative to those of the accepting orbital(s) of the excited complex are unfavorable for electron transfer.

DRu1

This was the first sequence selected for demonstrating clearly the presence of quenching and photo—cross-linking (Ortmans et al., 1999). The three guanines on both sides of the attachment site increase the probability to detect quenching conveniently. However, for this sequence the analyses of the emission decays have revealed to be the most complicated. The results from the treatment of the lifetimes data in Table 3 show that no long-lived component of 1.2 μs can be detected. On the basis of our modeling (Fig. 3 *A*) showing the stretching of the complex toward the 5′-direction, one may conclude that the complex in contact with the sixth basepair from the attachment site, is also close to the fifth and fourth basepair. This latter is a G-C pair in DRu1 toward the 5′-end but it is an A-T pair for a stretching toward the 3′-position. Therefore, the elongation in the 5′-direction should necessarily result in an emission quenching, whereas this is not obvious for the stretching toward the 3′-direction. Actually, when computer models are performed for the stretching toward the 3′-position (Fig. 3 *C*), the complex can reach only the third basepair from its tethering site, which is a guanine. This picture and the one with the stretching toward the 5′-end would thus account for the fact that no long-lived emission component is observed with sequence DRu1. However, it should be noticed that these computer models have to be considered with much care as they are very crude (Experimental section), and in any case, they should not be used for predictions.

CONCLUSIONS

The study of luminescence quenching of the different duplexes sequences in this work has highlighted several important factors that influence the primary process of DNA damage with Ru-labeled oligonucleotides. We have shown that static quenching is not present in these systems where the attached complex is not an intercalating species but adsorbs into the duplex grooves. A close contact between the linked complex and the guanines is needed for the electron transfer to take place, but even in that condition the process of hole injection remains rather slow as compared with the quenching by electron transfer between GMP and $[Ru(tap)_2(dip)]^{2+}$ free in solution. This slow rate indicates a bad orbital overlap between the complex acceptor and the guanine donor, because of steric hindrance brought by the linker. The results obtained by studying this first series of oligonucleotides duplexes will guide us for the design of new sequences that will refine the data concerning the parameters influencing the hole injection into these systems.

D. G.-F. thanks Prof. G. Orellana for helpful discussions; he is also grateful to the Complutense University of Madrid (Spain) for a post-doctoral grant. D. G.-F. and S. S. are grateful to the European T.M.R. program (ERBFMRXCT980226) for financial support. N. B., C. M. and A. K. D. are also grateful to the SSTC (PAI-IUAP 4/11 program) which has supported this work.

REFERENCES

Adamo, C., and V. Barone. 1998. Exchange functionals with improved long-range behavior and adiabatic connection methods without adjustable parameters: the mPW and mPW1PW models. *J. Chem. Phys.* 108:664–675.

Arkin, M. R., E. D. Stemp, S. Coates Pulver, and J. K. Barton. 1997. Long-range oxidation of guanine by Ru(III) in duplex DNA. *Chem. Biol.* 4:389–400.

Armitage, B. 1998. Photocleavage of nucleic acids. *Chem. Rev.* 98: 1171–1200.

Breen, A. P., and J. A. Murphy. 1995. Reactions of oxyl radicals with DNA. *Free Radic Biol Med* 18:1033–1077.

Cantor, C. R., and P. R. Schimmel. 1980. The conformation of biological macromolecules *and* The behavior of biological molecules. *In* Biophysical Chemistry. W. H. Freeman, San Francisco.

Carraway, E. R., J. N. Demas, and B. A. DeGraff. 1991. Luminescence quenching mechanism for microheterogeneous systems. *Anal. Chem.* 63:332–336.

Erkkila, K. E., D. T. Odom, and J. K. Barton. 1999. Recognition and reaction of metallointercalators with DNA. *Chem. Rev.* 99:2777–2795.

Frisch, M. J., G. W. Trucks, H. B. Schlegel, G. E. Scuseria, M. A. Robb, J. R. Cheeseman, V. G. Zakrzewski, J. A. Montgomery, Jr., R. E. Stratmann, J. C. Burant, S. Dapprich, J. M. Millam, A. D. Daniels, K. N. Kudin, M. C. Strain, O. Farkas, J. Tomasi, V. Barone, M. Cossi, R. Cammi, B. Mennucci, C. Pomelli, C. Adamo, S. Clifford, J. Ochterski, G. A. Petersson, P. Y. Ayala, Q. Cui, K. Morokuma, D. K. Malick, A. D. Rabuck, K. Raghavachari, J. B. Foresman, J. Cioslowski, J. V. Ortiz, A. G. Baboul, B. B. Stefanov, G. Liu, A. Liashenko, P. Piskorz, I. Komaromi, R. Gomperts, R. L. Martin, D. J. Fox, T. Keith, M. A. Al-Laham, C. Y. Peng, A. Nanayakkara, C. Gonzalez, M. Challacombe, P. M. Gill, B. Johnson, W. Chen, M. W. Wong, J. L. Andres, C. Gonzalez, M. Head-Gordon, E. S. Replogle, and J. A. Pople. 1998. Gaussian 98, Revision A.7, Gaussian, Inc., Pittsburgh PA.

García-Fresnadillo, D., Y. Georgiadou, G. Orellana, A. M. Braun, and E. Oliveros. 1996. Singlet-oxygen ($^1\Delta_g$) production by ruthenium complexes containing polyazaheterocyclic ligands in methanol and in water. *Helv. Chim. Acta.* 79:1222–1238.

García-Fresnadillo, D., M. D. Marazuela, M. C. Moreno-Bondi, and G. Orellana. 1999. Luminescent nafion membranes dyed with ruthenium(II) complexes as sensing materials for dissolved oxygen. *Langmuir.* 15: 6451–6459.

Gaspar, S. M., and G. B. Schuster. 1997. Intramolecular photoinduced electron transfer to anthraquinones linked to duplex DNA: the effect of gaps and traps on long-range radical cation migration. *J. Am. Chem. Soc.* 119:12762–12771.

Giese, B., S. Wessely, M. Spormann, U. Lindemann, E. Meggers, and M. E. Michel-Beyerle. 1999. On the mechanism of long-range electron transfer through DNA. *Angew. Chem. Int. Ed.* 38:996–998.

Hall, D. B., R. E. Holmlin, and J. K. Barton. 1996. Oxidative DNA damage through long-range electron transfer. *Nature.* 382:731–735.

Jacquet, L., R. J. Davies, A. Kirsch-De Mesmaeker, and J. M. Kelly. 1997. Photoaddition of $Ru(tap)_2(bpy)^{2+}$ to DNA: a new mode of covalent attachment of metal complexes to duplex DNA. *J. Am. Chem. Soc.* 119:11763–11768.

Jacquet, L., J. M. Kelly, and A. Kirsch-De Mesmaeker. 1995. Photoadduct between tris(1, 4, 5, 8-tetraazaphenanthrene)ruthenium(II) and guanosine monophosphate–a model for a new mode of covalent binding of metal complexes to DNA. *J. Chem. Commun.* 913–914.

Kelly, J. M., D. J. McConnell, C. OhUigin, A. Tossi, A. Kirsch-De Mesmaeker, A. Masschelein, and J. Nasielski. 1987. Ruthenium polypyridyl complexes: their interaction with DNA and their role as sensitisers for its photocleavage. *J. Chem. Soc. Chem. Commun.* 1821–1823.

Kelly, J. M., M. Feeney, L. Jacquet, A. Kirsch-De Mesmaeker, and J. P. Lecomte. 1997. Photoinduced electron transfer between ruthenium complexes and nucleotides or DNA. *Pure Appl. Chem.* 69:767–772.

Kirsch-De Mesmaeker, A., G. Orellana, J. K. Barton, and N. J. Turro. 1990. Ligand-dependent interaction of ruthenium(II) polypyridyl complexes with DNA probed by emission spectroscopy. *Photochem. Photobiol.* 52:461–472.

Kirsch-De Mesmaeker, A., J. P. Lecomte, and J. M. Kelly. 1996. Photoreactions of metal complexes with DNA, especially those involving a primary photo-electron transfer. *Topics Curr. Chem.* 177:25–76.

Lavery, R., K. Zakrzewska, and H. Sklenar. 1995. Jumna. *Comp. Phys. Commun.* 91:135–158.

Lecomte, J. P., A. Kirsch-De Mesmaeker, J. M. Kelly, A. B. Tossi, and H. Gorner. 1992. Photo-induced electron transfer from nucleotides to ruthenium-tris-1,4,5,8-tetraazaphenanthrene: model for photosensitized DNA oxidation. *Photochem. Photobiol.* 55:681–689.

Lecomte, J. P., A. Kirsch-De Mesmaeker, and G. Orellana. 1994. Photophysics of polyazaaromatic ruthenium(II) complexes interacting with DNA. *J. Phys. Chem.* 98:5382–5388.

Lecomte, J. P., A. Kirsch-De Mesmaeker, M. M. Feeney, and J. M. Kelly. 1995. Ruthenium(II) complexes with 1,4,5,8,9,12-hexaazatriphenylene and 1,4,5,8-tetraazaphenanthrene ligands: key role played by the photoelectron transfer in DNA cleavage and adduct formation. *Inorg. Chem.* 34:6481–6491.

Meggers, E., D. Kusch, M. Spichty, U. Wille, and B. Giese. 1998. Electron transfer through DNA in the course of radical-induced strand cleavage. *Angew. Chem. Int. Ed.* 37:459–462.

Molecular Simulations Inc. 1998. Insight II Modeling Environment. MSI, San Diego.

Moucheron, C., A. Kirsch-De Mesmaeker, and J. M. Kelly. 1997. Photoreactions of ruthenium(II) and osmium(II) complexes with deoxyribonucleic acid (DNA). *J. Photochem. Photobiol. B.* 40:91–106.

Moucheron, C., A. Kirsch-De Mesmaeker, and J. M. Kelly. 1998. Photophysics and photochemistry of metal polypyridyl and related complexes with nucleic acids. *Structure Bonding.* 92:163–216.

Nordén, B., P. Lincoln, B. Akerman, and E. Tuite. 1996. Probing of nucleic acids by metal ion complexes of small molecules. *In* Metal Ions in Biological Systems, Vol.33. A. Sigel and H. Sigel, editors. Marcel Dekker, New York. 177–252.

Ortmans, I. 1996. Photochimie de complexes métalliques homo- et hétéronucleaires en absence et en presence d'ADN. Ph.D. thesis. Free University of Brussels, Brussels. 119–147.

Ortmans, I., C. Moucheron, and A. Kirsch-De Mesmaeker. 1998. Ru(II) polypyridine complexes with a high oxidation power. Comparison between their photoelectrochemistry with transparent SnO_2 and their photochemistry with desoxyribonucleic acids. *Coord. Chem. Rev.* 168: 233–271.

Ortmans, I., S. Content, N. Boutonnet, A. Kirsch-De Mesmaeker, W. Bannwarth, J.-F. Constant, E. Defrancq, and J. Lhomme. 1999. Ru-labeled oligonucleotides for photoinduced reactions on targeted DNA guanines. *Chem. Eur. J.* 5:2712–2721.

Pyle, A. M., and J. K. Barton. 1990. Probing nucleic acids with transition metal complexes. *Progr. Inorg. Chem.* 38:413–475.

Saito, I., M. Takayama, H. Sugiyama, and K. Nakatani. 1995. Photoinduced DNA cleavage via electron transfer: demonstration that guanine residues located 5′ to guanine are the most electron-donating sites. *J. Am. Chem. Soc.* 117:6406–6407.

Saito, I., T. Nakamura, K. Nakatani, Y. Yoshioka, K. Yamagushi, and H. Sugiyama. 1998. Mapping of the hot spots for DNA damage by one-electron oxidation: efficiency of GG doublets and GGG triplets as a trap in long-range hole migration. *J. Am. Chem. Soc.* 120:12686–12687.

Sugiyama, H., and I. Saito. 1996. Theoretical studies of GG-specific photocleavage of DNA via electron transfer: significant lowering of ionization potential and 5′-localization of HOMO of stacked GG bases in B-form DNA. *J. Am. Chem. Soc.* 118:7063–7068.

Wan, C., T. Fiebig, S. O. Kelley, C. R. Treadway, J. K. Barton, and A. H. Zewail. 1999. Femtosecond dynamics of DNA-mediated electron transfer. *Proc. Natl. Acad. Sci. U.S.A.* 96:6014–6019.

Wan, C., T. Fiebig, O. Schiemann, J. K. Barton, A. H. Zewail. 2000. Femtosecond direct observation of charge transfer between bases in DNA. *Proc. Natl. Acad. Sci. U.S.A.* 97:14052–14055.

Xavier, M. P., D. García-Fresnadillo, M. C. Moreno-Bondi, and G. Orellana. 1998. Oxygen sensing in nonaqueous media using porous glass with covalently bound luminescent Ru(II) complexes. *Anal. Chem.* 70: 5184–5189.